On the Adsorption of Cr (VI) in Water by NiCoFe Ternary Metal-based LDHs

Yalu Zhao, Zhongwen Ou

Department of Chemistry & Material Engineering, Logistical Engineering University, Chongqing, 401311, China

Abstract

This paper prepares NO3- layer double hydroxides (LDHs) NiFe-LDHs, NiCoFe-LDHs and CoFe-LDHs by co-precipitation, studies the LDHs' adsorption of the heavy metal element Cr (VI) in water, and systematically explores the influence of the initial concentration of solution, the adsorption time and the pH value of the solution on the adsorption performance. The results indicate that the adsorption rate reaches 96.7% when the concentration of Cr (VI) solution is 2 mg/L, and reaches 30.22mg/g when the concentration of Cr (VI) solution is 10 mg/L. When the pH value of the solution is 5.5, the adsorption performance is the best, and the adsorption process can reach equilibrium in 30min. Thermodynamics and isothermal adsorption studies show that the adsorption process of Cr (VI) by NiCoFe-LDHs fits the Langmuir model and pseudo-second-order kinetics model. Thus, the adsorption process occurs on the adsorbent surface and the adsorption process is chemisorption.

Key words

NiCoFe-LDHs; preparation; adsorption; Cr(VI)

1. Introduction

Featuring high toxicity, long duration of pollution and degradation resistance, heavy metal wastewater poses a serious threat to the ecological environment and human health if it is

discharged arbitrarily. The wastewater from the metallurgical industry, metal surface treatment industry, hard chromium electroplating industry contains Cr(VI), which causes cancers, distortions and mutations [1]. The IARC has defined Cr(VI) as one of the carcinogenic metals [2]. According to WHO's regulations, the Cr(VI) content in wastewater shall not exceed 0.005mg/L [3]. Therefore, the removal of Cr(VI) in water is of great significance to ecological and environmental protection and drinking water safety. Currently, Cr(VI)-containing wastewater is mainly treated in the following ways: chemical precipitation, electrochemical method, ion exchange, electrolysis, photocatalytic reduction, biological treatment and adsorption [4-5]. The adsorption method has the advantages of simple operation, high processing efficiency, low cost, no secondary pollution, and adsorbent recyclability.

Layered double hydroxides (LDHs), commonly known as hydrotalcite-like compounds, feature unique lamellar structure, large specific surface area and excellent interlayer anion exchange ability. Thanks to the outstanding adsorption properties, LDHs are widely used in the field of wastewater treatment [6-8].

In the preliminary work of the lab, the research team studies the adsorption properties of NiFe-LDHs and CoFe-LDHs with different molar ratios of metal cations. The experiment reveals the best adsorption performance appears when the molar ratio of Ni:Fe to Co:Fe is 4: 1. Nevertheless, reviewing some literatures, the authors find that ternary metal-based LDH may have better adsorption properties than binary metal-based LDH. Based on the preliminary work, the research team adopts the co-precipitation method to prepare the NiCoFe ternary metal-based LDHs in which the molar ratio of divalent metal cations to trivalent metal cations is 4:1. The molar ratio of Ni: Co: Fe in the LDHs are 1:3:1, 2:2:1, and 3:1:1 respectively. The research team also prepares Ni4Fe1-LDHs and Co4Fe1-LDHs as the control groups. Then, the research team studies the morphology, chemical composition and crystal structure of the LDHs and probes into the adsorption process and the adsorption mechanism.

2. The experiment

2.1 The preparation of NiCoFe-based LDHs

The NiCoFe-LDHs are prepared by co-precipitation under nitrogen atmosphere. Firstly, the

research team dissolves $Ni(NO_3)_2 \cdot 6H_2O$, $Co(NO_3)_2 \cdot 6H_2O$ and $Fe(NO_3)_3 \cdot 9H_2O$ (99%; Shanghai Aladdin Bio-Chem Technology Co., Ltd.), in which the molar ratio of Ni: Co: Fe is 1:3:1, 2:2:1 and 3:1:1 respectively, in 40mL of deionized water (total cation concentration: 1 mol/L), and adds the above saline solution dropwise to a solution which is being stirred rapidly in a magnetic stirrer (200 mL, 0.5 mol/L; Chongqing Chuandong Chemical Group Co., Ltd.). Then, the team places the resulting suspension in a water bath of 338K, stirs the suspension for 18h, and washes it with deionized water to neutral. After that, the team centrifuges the resulting suspension, removes the supernatant, and dries the lower precipitation in a vacuum oven at 338 K for 24 h to obtain the sample NiCoFe-LDHs. Finally, the team grinds the product and stores it in a glass container. Three types of NiCoFe-LDHs are prepared, namely $Ni_3Co_1Fe_1$-LDHs, $Ni_2Co_2Fe_1$-LDHs, and $Ni_1Co_3Fe_1$-LDHs. All the reagents are of analytical grade, and all the solutions are prepared from deionized water. Ni_4Fe_1-LDHs and Co_4Fe_1-LDHs are prepared by the same method as reference.

2.2 The adsorption experiment

At room temperature, the team adds $K_2Cr_2O_7$ into the deionized water, and prepares $Cr_2O_7^{-}$ solutions of different concentrations (100mL for each concentration). Then, the team takes 20mg of the prepared LDHs powder and places it into the $Cr_2O_7^{-}$ solutions of different initial concentrations. The adsorption experiment should take place in the shade and the pH value should be adjusted by HCl and NaOH. Besides, the team should stir the mixture in the magnetic stirrer at a constant speed, and take about 5mL of mixture at regular intervals for centrifugal separation. After taking the supernatant, the team uses inductively coupled plasma emission spectrometry (ICP) to detect the concentration variation of the supernatant, and calculates the adsorption rate and adsorption capacity at equilibrium according to the following empirical formulas:

$$q_e = \frac{(c_0 - c_e)V}{m}$$

(1)

$$R = \frac{c_0 - c_t}{c_0} \times 100\%$$

(2)

In the above formulas, c_0(mg/L) and c_e(mg/L) are the initial concentration and equilibrium concentration of $Cr_2O_7^{-}$ solution, c_t(mg/L) is the concentration of Cr (VI) solution at time t, m(g) is the mass of the adsorbent, and V(L) is the volume of the solution.

2.3 The characterization method

The concentration of Cr(VI) in the solution and the content of NiCoFe in the prepared LDHs powder are measured by inductively coupled plasma atomic emission spectrometry (iCAP-6000 Series). The x-ray diffraction patterns of the prepared LDHs powder are obtained by X-ray diffractometer (Bruker D8 Advance with Cu Kα 99 radiation). The FT-IR spectra are obtained by Fourier transform infrared spectroscopy (FT-IR, Nicolet is50). The morphology of LDHs is observed by scanning electron microscopy (SEM, JEOL). The thermogravimetric analysis (TGA) is performed with a TGA/DSC 105 1/1100 LF in a nitrogen atmosphere at a rate of 10°C/min. The specific surface area and pore diameter of the samples are measured using a conventional N_2 adsorption-desorption curve at a 77 with the ASAP 2020 pore distribution analyzer manufactured by Max.

3. Results and discussion
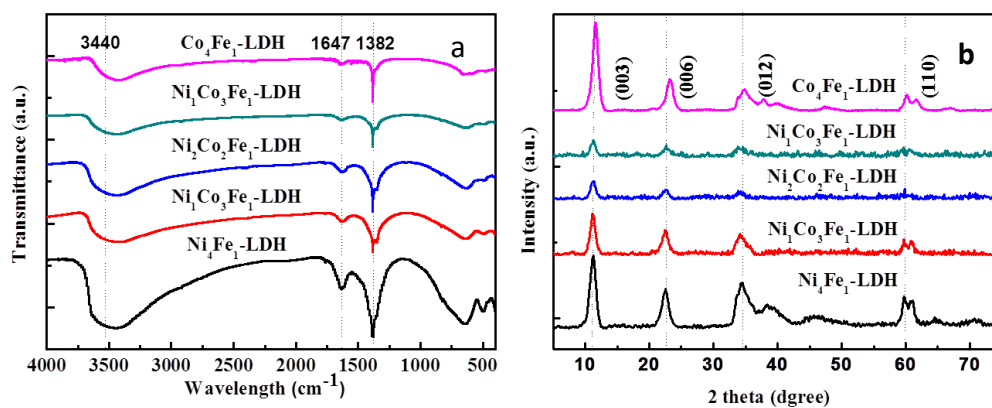
3.1. Characterization of LDHs

Fig. 1 (a) FT-IR spectrograms and (b) XRD spectrograms of NiFe-LDHs, NiCoFe-LDHs, and CoFe-LDHs.

Figure 1(a) presents the IR spectra of NiFe-LDHs, NiCoFe-LDHs and CoFe-LDHs.

The infrared active vibrations of LDHs can be divided into three categories: molecular vibration of hydroxyl, lattice vibration of octahedron, and the interlayer vibration of anions [9]. The strong absorption peaks at 3,440 cm^{-1} and 1,647 cm^{-1} are resulted from the vibrations of the water molecules and the OH bending and stretching vibrations in the OH-OH bond, indicating the

existence of hydroxide radicals on hydrotalcite layer and crystal waters between the layers. The strong absorption peak at 1,382 cm^{-1} is the vibration absorption peak of NO^{3-} in NiCoFe-LDHs [10]. The peak below 1,000 cm^{-1} is the lattice vibration peak of M-O and M-O-M in the hydrotalcite-like layer [11].

Figure 1(b) displays the XRD spectrograms of LDHs. As shown in the figure, the main diffraction peaks of NiFe-LDHs, NiCoFe-LDHs and CoFe-LDHs are sharp and narrow, with stable baseline and symmetrical peak shape, indicating that the purity and crystallinity of the products are very high. For the sample NiFe-LDHs, NiCoFe-LDHs and CoFe-LDHs, distinct characteristic diffraction peaks are observed when the incident angle is at 11°, 22°, 34° and 60° respectively. The characteristic peaks correspond to the crystal face diffraction peaks of traditional hydrotalcite at d(003), d(006), d(012) and d(110), indicating that the samples have the typical lamellar crystal structures of LDHs.[12] The team evaluates the contents of the divalent metal and trivalent metal by ICP. The results show that the molar ratio of divalent metal cations to trivalent metal cations in Ni_4Fe_1-LDHs, Ni_3Co_1Fe1-LDH$_s$, Ni_2Co_2Fe1-LDHs, $Ni_1Co_3Fe_1$-LDHs and Co_4Fe_1-LDHs is 4.2, 3.8, 4, 4 and 4.3 respectively. This means the ratio of metal ions in the prepared samples is consistent with the predicted ratio.
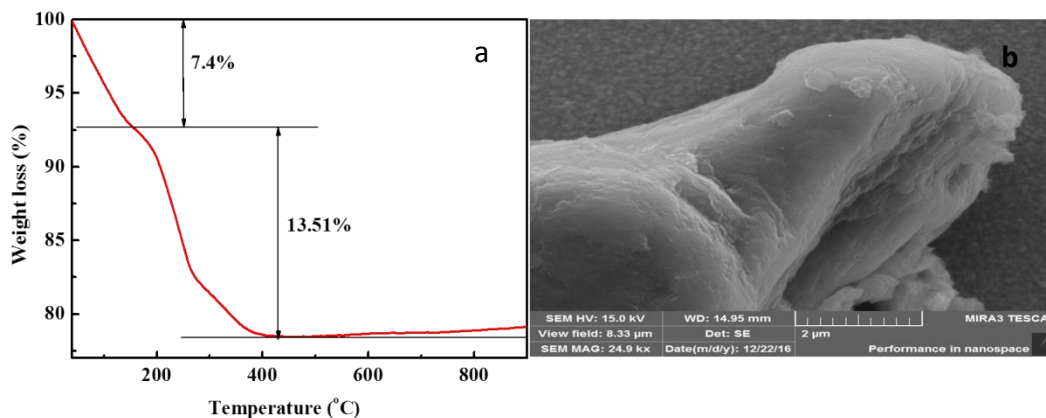

Fig. 2 (a) TGA spectrograms and (b) SEM images of $Ni_1Co_3Fe_1$-LDHs

The thermogravimetric analysis of NiCoFe-LDHs is shown in Figure 2(a). With the increase in temperature, the samples go through a two-stage weight loss process. In the first stage, the temperature rises from 40°C to 165°C and the samples lost 7.4% of weight. The weight loss is mainly caused by the disappearance of water molecules and inter-laminar water molecules. As the temperature continues to rise, the second stage begins. When the temperature reaches the range between 165°C and 435°C, the mass loss of the samples is about 13.51%, which is resulted from

the removal of nitrate ions and dehydroxylation between layers [13].

Figure 2(b) illustrates the morphology and nanostructures of NiCoFe-LDHs, which are observed with the SEM. The SEM images show that the NiCoFe-LDHs are in the form of lamellar stacks, featuring the typical morphology of LDHs synthetized by co-precipitation. The random polymerization, aggregation and random stacking of microcrystals affect the specific surface area, pore diameter and charge density of the material, and thereby reducing the adsorption performance of the material.

Table 1. The specific surface areas and pore characteristics of NiFe-LDHs, NiCoFe-LDHs and CoFe-LDHs

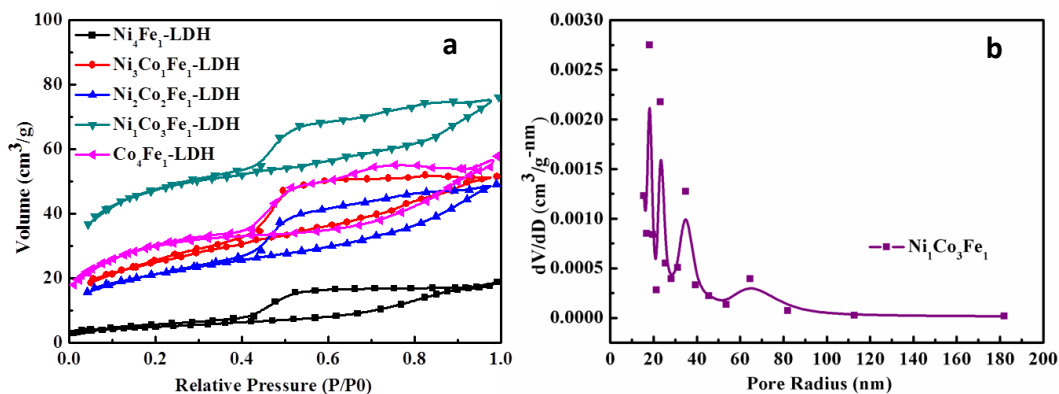| Samples	Average pore diameter(nm)	Pore volume(cm^3/g)	Surface area(m^2/g)
Ni_4Fe_1	1.8	0.032	17.847
$Ni_3Co_1Fe_1$	15.518	0.049	72.967
$Ni_2Co_2Fe_1$	16.725	0.048	87.259
$Ni_1Co_3Fe_1$	18.112	0.049	160.908
Co_4Fe_1	8.4	0.047	108.84

Fig. 3 (a) N$_2$ absorption-desorption isotherms of NiFe-LDHs, NiCoFe-LDHs, and CoFe-LDHs, (b) pore diameter distribution of Ni$_1$Co$_3$Fe$_1$-LDHs

See Figure 3 for the specific surface area and pore characteristics of NiCoFe-LDHs nanomaterials. In accordance with the IUPAC classification of adsorption isotherms, the isothermal adsorption curves of the five types of samples in Figure 3(a) are typical Type IV isothermal adsorption curves, coupled with H3-type hysteresis loop. Thus, all the materials are of mesoporous structure with lamellar pores [14], and are possible to have mesopores. As listed in Table 1, the specific surface area of Ni$_1$Co$_3$Fe$_1$-LDHs is 160.908 m^2/g, while that of the other samples falls between 17 and 108 m^2/g. Besides, Ni$_1$Co$_3$Fe$_1$-LDHs has an average pore diameter

of 18.112nm, the largest among all five samples. Figure 3(b) shows the distribution of pore diameters of $Ni_1Co_3Fe_1$-LDHs. It proves that $Ni_1Co_3Fe_1$-LDHs is a mesoporous material. Since the specific surface area and pore diameter have a great impact on the adsorption performance of the material, it is deducted that $Ni_1Co_3Fe_1$-LDHs has the best adsorption properties among the prepared samples.

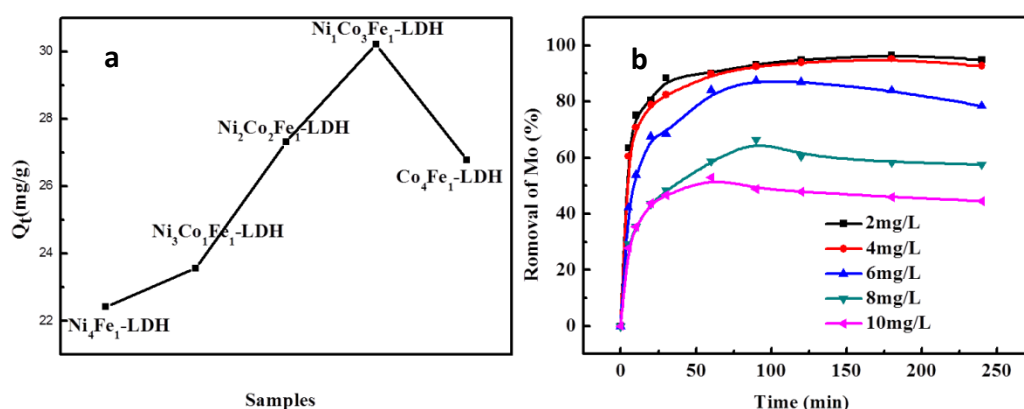## 3.2 Adsorption of Cr (VI) by LDHs

Fig. 4 (a) The amounts of 10mg/L chromium solution adsorbed by NiFe-LDHs, NiCoFe-LDHs, and CoFe-LDHs, (b) The adsorption rates of different concentrations of Cr_2O^{7-} solution by $Ni_1Co_3Fe_1$-LDHs over time

The chemical composition of the LDH layers depends on the ratio of metallic elements in the LDHs, which in turn affects the chemical properties of the layers and the interlayer charge density. As a consequence, the adsorption of Cr(VI) is also greatly affected by the ratio. In view of this, the research team adds 20mg of LDHs powder into Cr_2O^{7-} solution with initial mass concentration of 10mg/L. When the reaction reaches equilibrium, the team uses the ICP to measure the concentration of the solution, and calculates the saturated adsorption capacity. Figure 4(a) displays the saturated adsorption capacities of the five samples on Cr(VI). The amounts of Cr(VI) adsorbed by Ni_4Fe_1-LDHs, Ni_3Co_1Fe1-LDHs, $Ni_2Co_2Fe_1$-LDHs, $Ni_1Co_3Fe_1$-LDHs and Co_4Fe_1-LDHs are respectively 22.42 mg/g, 23.57 mg/g, 27.32 mg/g, 31.07 mg/g and 26.78mg/g. Among them, $Ni_1Co_3Fe_1$-LDHs can adsorb 31.07 mg/g of Cr_2O^{7-} at the maximum, indicating that the sample boasts the strongest adsorption capacity. This is probably attributable to the fact that $Ni_1Co_3Fe_1$-LDHs has the largest pore diameter and specific surface area among the five samples. As the diffusion channel of the adsorbed molecules, the pore diameter has an effect on the adsorption rate. The larger the pore size is, the faster the adsorption rate [15]. Similarly, the

adsorption rate of Cr(VI) is also affected by the specific surface area. The larger the specific surface area, the more active adsorption sites in the aqueous solution [16]. That is why $Ni_1Co_3Fe_1$-LDHs has the strongest adsorption capacity. The research team digs deeper into the adsorption of Cr(VI) by $Ni_1Co_3Fe_1$-LDHs. Figure 4(b) presents the adsorption rates of different concentrations (2-10 mg/L) of Cr_2O^{7-} solution by $Ni_1Co_3Fe_1$-LDHs over time. As illustrated by the adsorption curves, the adsorption reaction develops faster in the first 30min, which echoes with the reaction characteristics of LDHs. At the beginning of the reaction, there are a lot of active adsorption sites on the surface of $Ni_1Co_3Fe_1$-LDHs. Over the time, the unoccupied active sites are increasingly difficult to occupy due to the repulsion between the solute molecules. Thus, the adsorption rate gradually decreases [17]. The adsorption reaction reaches equilibrium at 2h, indicating that $Ni_1Co_3Fe_1$-LDHs is saturated with Cr(VI). For the Cr_2O^{7-} solution with initial concentration of 2mg/L, the adsorption rate is 96.7%. The amounts of Cr(VI) adsorbed by other hydrotalcite compounds are shown in Table 2. It can be inferred that the adsorption capacity of NiCoFe-LDHs is higher than that of other binary metal-based LDHs. With such an excellent adsorption performance, the NiCoFe-LDHs has great potential in sewage treatment.

Table 2. Comparison of maximum adsorption capacities of various adsorbents for Cr(VI)

Adsorbent	q_m(mg/g)	References
MgAl-LDH	17	[18]
MgAlCe-LDH	31.1	[19]
NiFe-LDHs	26.78	[20]
CoFe-LDHs	22.42	[16]
NiCoFe- LDHs	30.22	This study

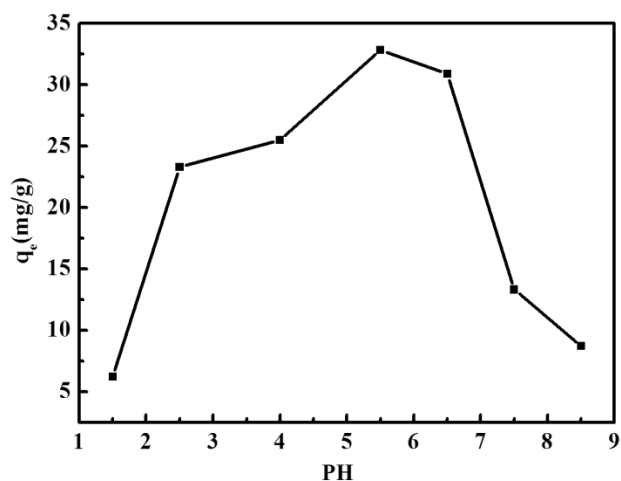**3.3 The influence of solution pH value on the adsorption of Cr(VI)**

Fig. 5 The influence of solution pH value on the adsorption of Cr(VI)

The pH value of the solution is an important influencing factor of the adsorption performance. To explore the influence of the pH value of the solution on the adsorption of Cr(VI), the research team prepares several 10mg/L Cr_2O^{7-} solutions, and adjusts the pH value to 1.5, 2.5, 4.0, 5.5, 6.5, 7.5 and 8.5 respectively. Adding 20mg of adsorbent, the team lets the solutions to react at room temperature for 3h. The experiment results are shown in Figure 5. According to the figure, the adsorption amount is relatively stable when the pH value is between 5 and 7. The influence of the solution pH on the adsorption of Cr(VI) can be explained in the following two aspects. On the one hand, the form of Cr(VI) in aqueous solution is affected by pH value. It exists in the form of CrO_2^{-4} in alkaline environment, and $HCrO^{4-}$ and $Cr_2O_2^{-7}$ in acidic environment [21]. With a lower adsorption free energy than CrO_2^{-4}, $HCrO^{4-}$ is easier to adsorb than CrO_2^{-4} [22]. Moreover, the chromium content of $Cr_2O_2^{-7}$ is twice that of CrO_2^{-4}. Thus, the amount of adsorbed Cr(VI) is higher in acidic environment (pH<7). On the other hand, when pH value is less than 2, the Cr(VI) in water is in the form of H_2CrO_4 [23], which cannot exchange with the anions between LDH layers. Therefore, when the PH value of the solution is between 5 and 7, a high amount of Cr(VI) is adsorbed by LDH.
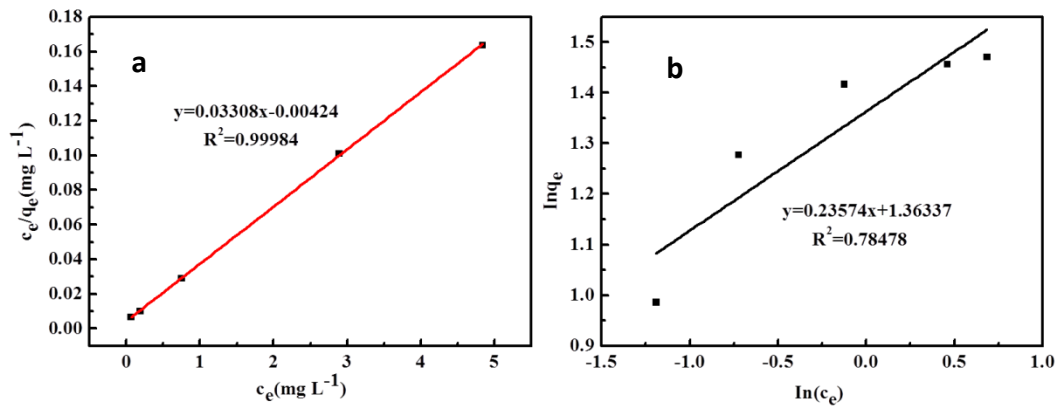
3.4 On the thermodynamics of adsorption

Fig. 6 Adsorption isotherms of Cr by $Ni_1Co_3Fe_1$-LDH based on different models: (a) Langmuir model, (b) Freundlich model

Isothermal adsorption curve reveals how the adsorbed molecules are dispersed in the solid and liquid phases during adsorption. The research team uses the Langmuir model and the Freundlich model to analyze the adsorption data for different initial mass concentrations of Cr_2O^{7-} [24-25].

The formula of Langmuir model is:

$$c_e / q_e = 1 / q_m k_L + c_e / q_m \tag{3}$$

The formula of Freundlich model is:

$$Inq_e = InK_F + 1 / nInc_e \tag{4}$$

In the formulas, q_m is the Cr_2O^{7-} adsorption capacity of NiCoFe-LDHs at the adsorption equilibrium and the maximum capacity, mg/g; K_L is the Langmuir constant, L/mg; K_F is a Freundlich constant, $mg^{1-1/n}L^{1/n}g^{-1}$; 1/n is also a Freundlich constant, which is related to the adsorption intensity. It can be seen from Figure 6 that the adsorption data agree well with the Langmuir model. By fitting analysis, it is obtained that the correlation coefficient $R^2 = 0.99984$, indicating that Cr(VI) is easily adsorbed on the surface of $Ni_1Co_3Fe_1$-LDHs. The Langmuir model assumes that the adsorption process occurs on a homogeneous surface [26]. The model demonstrates that the adsorption is a surface monolayer adsorption that occurs on the surface of the adsorbent. With this model, it is calculated that the maximum theoretical adsorption capacity of $Ni_1Co_3Fe_1$-LDHs on Cr(VI) is 30.22mg/g, which is close to the experimental result of 31.07.
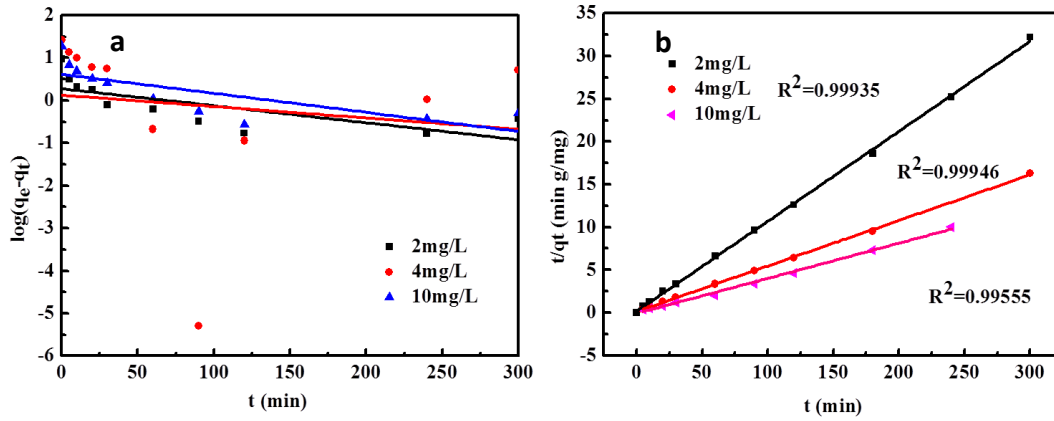
3.5 On the kinetics of adsorption

Fig. 7 The pseudo-first-order kinetics model (a) and pseudo-second-order kinetics model (b) for

the Cr adsorption of $Ni_1Co_3Fe_1$ –LDHs

Adsorption kinetics model describes the adsorption rate and provides data to assist the study of adsorption mechanisms and adsorption processes. Common kinetics models include the pseudo-first-order kinetics model and the pseudo-second-order kinetics model [27-28].

The pseudo-first order kinetics model is expressed as:

$$\ln(q_e - q_t) = \ln q_e - \frac{k_1}{2.302}t \tag{5}$$

The pseudo-second order kinetics model is expressed as:

$$\frac{t}{q_t} = \frac{1}{k_2 q_e^2} + \frac{t}{q_e} \tag{6}$$

In the formulas, k_1 and k_2 are respectively the adsorption rate constants of the pseudo-first-order kinetics model and the pseudo-second-order kinetics model (min-1), (mg/g•min). The data of q_t and t are obtained from the experiment, and k_1 and k_2 are calculated by fitting the the intercept and slope in the figure.[29] As shown in Figure 7, the correlation coefficient R^2 (> 0.999) of the pseudo-second-order kinetics model is larger than that of the pseudo-first-order kinetics model, indicating that the experimental data better fit the pseudo-second-order kinetics model. Hence, the adsorption process is chemisorption.[30-31]

4. Conclusion

1) The research team prepares five types of LDHs in which the molar ratio of divalent metal

cations to trivalent metal cations is 4:1 by co-precipitation. All of the LDHs have good adsorption performances. Among them, the ternary metal-based $Ni_1Co_3Fe_1$-LDHs boasts the largest specific surface area, average pore diameter and the adsorption performance.

2) The isothermal adsorption curves show that the adsorption of Cr(VI) by NiCoFe-LDHs is in accordance with the Langmuir model. Thus, the adsorption is surface monolayer adsorption.

3) The study on adsorption kinetics reveals that the adsorption of Cr(VI) by NiCoFe-LDHs can be described by the pseudo-second-order kinetic model, which indicates that the adsorption process is chemisorption and the adsorption rate is affected by Cr(VI) concentration.

References

1. J. Kotaś, Z. Stasicka. Chromium occurrence in the environment and methods of its speciation. 2000, Environmental pollution, vol. 107, no. 3, pp. 263-283.

2. P.C.C Faria, J.J.M Órfão, M.F.R Pereira, Adsorption of anionic and cationic dyes on activated carbons with different surface chemistries, 2004, Water Res, vol. 38, pp. 2043-2052.

3. A. Seron, F. Delorme, Synthesis of layered double hydroxides (LDHs) with varying pH: A valuable contribution to the study of Mg/Al LDH formation mechanism, 2008, J. Phys Chem. Solids vol. 69, pp. 1088-1090.

4. C.E. Barrera-Díaz, V. Lugo-Lugo, B. Bilyeu. A review of chemical, electrochemical and biological methods for aqueous Cr (VI) reduction, 2012, Journal of hazardous materials, vol. 223, pp. 1-12.

5. W. Wang, J. Zhou, G. Achari, et al. Cr (VI) removal from aqueous solutions by hydrothermal synthetic layered double hydroxides: Adsorption performance, coexisting anions and regeneration studies, 2014, Colloids and Surfaces A: Physicochemical and Engineering Aspects, vol. 457, pp. 33-40.

6. Y. Wang, H. Gao. Compositional and structural control on anion sorption capability of layered double hydroxides (LDHs), 2006, Journal of Colloid and Interface Science, vol. 301, no. 1, pp. 19-26.

7. X. Guo, F. Zhang, Q. Peng, et al. Layered double hydroxide/eggshell membrane: An inorganic biocomposite membrane as an efficient adsorbent for Cr (VI) removal, 2011, Chemical Engineering Journal, vol. 166. no. 1, pp. 81-87.

8. S. He, Y. Zhao, M. Wei, et al. Preparation of oriented layered double hydroxide film using electrophoretic deposition and its application in water treatment, 2011, Industrial & Engineering Chemistry Research, vol. 50, no. 5, pp. 2800-2806.

9. P. Kuśtrowski, D. Sułkowska, L. Chmielarz, et al. Influence of thermal treatment conditions on the activity of hydrotalcite-derived Mg–Al oxides in the aldol condensation of acetone, 2005 Microporous and Mesoporous Materials, vol. 78, no. 1, pp. 11-22.

10. K. Xu, G. Chen, J. Shen. Exfoliation and dispersion of micrometer-sized LDH particles in poly (ethylene terephthalate) and their nanocomposite thermal stability, 2013, Applied Clay Science, vol. 75, pp. 114-119.

11. F.B.D. Saiah, B.L. Su, N. Bettahar. Nickel–iron layered double hydroxide (LDH): textural properties upon hydrothermal treatments and application on dye sorption, 2009, Journal of Hazardous Materials, vol. 165, no. 1, pp. 206-217.

12. Z.P. Xu, H.C. Zeng, Abrupt Structural Transformation in Hydrotalcite-like Compounds $Mg_{1-x}Al_x(OH)_2(NO_3)_x \cdot nH_2O$ as a Continuous Function of Nitrate Anions, J. Phys. Chem. B 105(2001) 1743-1749.

13. K. Xu, G. Chen, J. Shen, Exfoliation and dispersion of micrometer-sized LDH particles in poly (ethylene terephthalate) and their nanocomposite thermal stability, 2013, Appl. Clay Sci. vol. 75, pp. 114-119.

14. B. Tanhaei, A. Ayati, M. Lahtinen, et al. Preparation and characterization of a novel chitosan/Al2O3/magnetite nanoparticles composite adsorbent for kinetic, thermodynamic and isotherm studies of Methyl Orange adsorption. 2015, Chemical Engineering Journal, vol. 259, pp. 1-10.

15. C. Pelekani, V.L. Snoeyink. Competitive adsorption between atrazine and methylene blue on activated carbon: the importance of pore size distribution, 2000, Carbon, vol. 38, no. 10, pp. 1423-1436.

16. F. Ling, L. Fang, Y. Lu, et al. A novel CoFe layered double hydroxides adsorbent: High adsorption amount for methyl orange dye and fast removal of Cr (VI), 2016, Microporous and Mesoporous Materials, vol. 234, pp. 230-238.

17. Yang Z, Ji S, Gao W, et al. Magnetic nanomaterial derived from graphene oxide/layered double hydroxide hybrid for efficient removal of methyl orange from aqueous solution . Journal of colloid and interface science, 2013, 408: 25-32.

18. N.K. Lazaridis, T.A. Pandi, K.A. Mati. Chromium (VI) Removal from Aqueous Solutions by Mg− Al− CO3 Hydrotalcite: Sorption− Desorption Kinetic and Equilibrium Studies. 2004, Industrial & engineering chemistry research, vol. 43, no. 9, pp. 2209-2215.

19. W.S. Chen. Synthesis and characterization of Mg/Al/Ce (Ⅳ)-Layered Double Hydroxide and study on adsorption of Cr(IV) from aqueous solutions by its mixed oxides. Shandong University, 2009

20. Y. Lu, B. Jiang, L. Fang, et al. High performance NiFe layered double hydroxide for methyl orange dye and Cr (VI) adsorption . Chemosphere, 2016, 152: 415-422.

21. A. Benhammou, A. Yaacoubi, L. Nibou, et al. Chromium (VI) adsorption from aqueous solution onto Moroccan Al-pillared and cationic surfactant stevensite, 2007, Journal of hazardous materials, vol. 140, no. 1, pp. 104-109.

22. C.H. Weng, J.H. Wang, C.P. Huang. Adsorption of Cr (VI) onto TiO2 from dilute aqueous solutions, 1997, Water Science and Technology, vol. 35, no. 7, pp. 55-62.

23. S. Zhou, F. Liu, Q. Zhang, et al. Preparation of polyacrylonitrile/ferrous chloride composite nanofibers by electrospinning for efficient reduction of Cr (VI), 2015, Journal of nanoscience and nanotechnology, vol. 15, no. 8, pp. 5823-5832.

24. I. Langmuir. The adsorption of gases on plane surfaces of glass, mica and platinum. 1918, Journal of the American Chemical Society, vol. 40, no. 9, pp. 1361-1403.

25. S. Srisuda, B. Virote. Adsorption of formaldehyde vapor by amine-functionalized mesoporous silica materials, 2008, Journal of Environmental Sciences, vol. 20, no. 3, pp. 379-384.

26. X. Ruan, Y. Chen, H. Chen, et al. Sorption behavior of methyl orange from aqueous solution on organic matter and reduced graphene oxides modified Ni–Cr layered double hydroxides. 2016, Chemical Engineering Journal, vol. 197, pp. 295-303.

27. M. Toor, B. Jin. Adsorption characteristics, isotherm, kinetics, and diffusion of modified natural bentonite for removing diazo dye, 2012 Chemical Engineering Journal, vol. 187, pp. 79-88.

28. V. Belessi, G. Romanos, N. Boukos, et al. Removal of Reactive Red 195 from aqueous solutions by adsorption on the surface of TiO2 nanoparticles. 2009, Journal of Hazardous Materials, vol. 170, no. 2, pp. 836-844.

29. Z. Li, B. Yang, S. Zhang, et al. A novel approach to hierarchical sphere-like ZnAl-layered double hydroxides and their enhanced adsorption capability, 2014, Journal of Materials Chemistry A, vol. 26, no. 2, pp. 10202-10210.

30. W.J. Weber, J.C. Morris. Kinetics of adsorption on carbon from solution, 1963, Journal of the Sanitary Engineering Division, vol. 89, no. 2, pp. 31-60.

31. B.H. Hameed, A.L. Ahmad, K.N.A. Latiff. Adsorption of basic dye (methylene blue) onto activated carbon prepared from rattan sawdust, 2007, Dyes and Pigments, vol. 75, no. 1, pp. 143-149.